

SAGA-HE-106
 KEK-Preprint 96-83
 KEK-CP-048
 July 1996
 (Revised: August 1996)

Single-W production to test triple gauge boson couplings at LEP

Toshio Tsukamoto [†]

Department of Physics, Saga University, Saga 840, Japan

Yoshimasa Kurihara

KEK, National Laboratory for High Energy Physics, Ibaraki 305, Japan

Abstract

We present a study of single-W production ($e^+e^- \rightarrow e^-\bar{\nu}_e W^+$) as a new probe of the anomalous couplings at the LEP energy region. We introduce simple cuts to separate the single-W process from W-pair production and have performed cross-section calculations using 4-fermion generator “grc4f”. The cross-section of the single-W process is found to be large enough to detect at LEP experiments in the near future. In addition, a high sensitivity to the anomalous coupling of the $WW\gamma$ vertex is expected since the amplitude of the $WW\gamma$ diagram makes a dominant contribution in this process. We have found that the cross-section measurement of the single-W process in the LEP2 energy region can give complementary bounds on the anomalous couplings to those obtained from W-pair analysis.

(*To appear in Physics Letters B*)

[†]E-mail address: ttoshio@cc.saga-u.ac.jp

1 Introduction

Recent high precision measurements performed at LEP and SLC have clarified that the fermion-gauge boson couplings are amazingly well described by the Standard Model (SM). On the other hand, the gauge sector of the Standard Model is still poorly measured. The non-abelian self couplings of gauge bosons are the most direct consequences of the $SU(2) \times U(1)$ gauge symmetry and the couplings of Triple Gauge boson Couplings (TGC) are uniquely determined by the Standard Model. Any deviation of these couplings from their expectation would indicate physics beyond the Standard Model. While TGCs only enter through loop corrections at LEP1 energy, a direct confirmation of these couplings can be made at LEP2.

Prior to the actual startup of LEP2, a number of studies have already been made to find possible ways to probe non-standard $WW\gamma$ and WWZ couplings [1]. Most studies up-to now have focused on the process $e^+e^- \rightarrow W^+W^-$. Although this process is anticipated to give a good sensitivity to the anomalous couplings, it suffers from the disadvantage that one cannot disentangle the effects of $WW\gamma$ and WWZ couplings. Especially, the gauge cancellations between γ , Z^0 and neutrino exchange graphs are still not fully operative at LEP2 energy region, hence, only the interference effects between different TGCs dominate. One has to utilise the angular dependence and correlations of the decay products as much as possible to isolate different linear combination of WWV ($V = \gamma, Z$) couplings.

One way to avoid such complications is to use the reaction $e^+e^- \rightarrow \nu\bar{\nu}\gamma$ where only the structure of the $WW\gamma$ coupling can be studied [2, 3]. The expected sensitivity limits are, however, substantially weaker at the energy region accessible to LEP [2] because the diagram involved in this channel is WW fusion type.

Another candidate is a single-W process: $e^+e^- \rightarrow e^-\bar{\nu}_e W^+$. This process is not well studied so far for LEP. Pioneering works [4] are done to include this ‘single-W’ process for the test of TGC. Unfortunately, relatively large polar angle of the out-going electron is demanded in order to avoid collinear singularities in the calculation in [4]. The contribution of real “single-W” is essentially suppressed as a result. In addition, because no separation is made against W-pair production in [4], the estimated sensitivity is dominated by W-pair contribution above the WW threshold.

In this letter we propose a new probe of the $WW\gamma$ vertex using $e^+e^- \rightarrow e^-\bar{\nu}_e W^+$ process where the electron escapes down the beam pipe. We suggest the selection criteria for single-W production and present the anticipated sensitivity to the anomalous TGCs.

2 Single-W production

At the energy region of LEP2 and above, four-fermion final state can, in general, be produced by double (heavy boson) resonant diagrams, single resonant diagrams or non-resonant diagrams. Single-W processes include $e^+e^- \rightarrow \ell^-\bar{\nu}_\ell W^+$ where ℓ can be either an electron or a muon, and W decays into two fermions. The electron case is attractive since t -channel diagrams also exist. For example, the diagram involved in $e^+e^- \rightarrow e^-\bar{\nu}_e \mu^+ \nu_\mu$ can be grouped into the s -channel (figure 1) and t -channel classes (figure 2), each group forms a gauge invariant set. Among the t -channel diagrams, the γ - W process (the first row in figure 2) give the dominant contribution. Even below the WW threshold, a significant contribution is expected from the γ - W - W diagram (the second graph in figure 2).

In order to enhance the t -channel contribution, we need to require the outgoing electron to be within a small angle. This cut causes several problems for the cross-section calculation. First of all, the matrix element needs to keep even the electron mass finite throughout the calculation to avoid a singularity at small electron polar angle (θ_{e^-}). It should be noted that, although a number of event generators for four-fermion processes are available now [5], some approximation, including zero mass of fermions, are often introduced in order to cope with the complexity of the calculation. Secondly, the gauge violating term due to the introduction of the finite width of W is found to blow up at small θ_{e^-} [6], and stops one from obtaining reliable cross-section as a result. This problem can, however, be avoided by several methods [7, 8] and the results of each scheme are found to be consistent [8]. The third problem is a technical one. Since a large cancellation between the γ - W processes is expected in the unitary gauge, one has to pay attention to the calculation of the cross-section especially when a numerical integration is used. This can be avoided if one takes an efficient gauge.

Here we use “grc4f” [9] for the calculation. In this package, all the fermion masses are properly taken into account in the helicity amplitude

(CHANEL [10]). A numerical integration with multi-dimensional phase space is done by BASES [11]. The gauge violation due to the finite width of the W is cured by subtracting the terms which satisfy the Ward identity, from the electron current [7]. This method also benefits the stability of the numerical integration since each amplitude is safely kept close to unity. One can thus perform a cross-section calculation reliably even without a cut on the electron polar angle. A kinematics suitable for the single- W process is completely different from that for W -pairs. The package “grc4f” incorporates another set of special kinematics aimed at studying single W processes. The result presented here have been obtained using the following set of parameters:

$$\begin{aligned} M_Z &= 91.189 \text{GeV}, & \Gamma_Z &= 2.497 \text{GeV}, \\ M_W &= 80.23 \text{GeV}, & \Gamma_W &= 2.034 \text{GeV}, \\ \alpha &= 1/128.07, & \sin^2\theta_W &= 1 - (M_W^2/M_Z^2). \end{aligned}$$

For the radiative corrections, the electron structure function at $\mathcal{O}(\alpha^2)$ [12] is convoluted with the cross-section for a primary process. Hard emitted photons with finite transverse momentum may, in general, distort the direction of the final fermions. This effect could not be negligible for the processes with the electron (positron) in the final state, for example, the t -channel classes of $e^+e^- \rightarrow e^-\bar{\nu}_e\mu^+\nu_\mu$, due to a steep forward-peak of their angular distribution. In our approximation, initial state photons are radiated along the beam axis, and the effect stated above is not taken into account. However the global correction of initial state radiation is still useful to estimate an experimental sensitivity for TGCs. For the future precise measurements of TGCs, more complete treatment for the radiative corrections is desired.

3 Experimental signature

We mainly focus on the $e^+e^- \rightarrow e^-\bar{\nu}_e\mu^+\nu_\mu$ process in this letter since the signature is very clean from an experimental point of view. Once the W -pair threshold opens, one has to discriminate single- W from WW . This can be done very simply by demanding the electron travels down to the beam pipe. We use the following cuts on the polar angles for the electron and the muon.

$$\theta_{e^-} < 35 \text{ mrad} \quad \text{and} \quad |\cos\theta_{\mu^+}| < 0.95. \quad (1)$$

The resulting event signature is “single muon”. In order to demonstrate how these cuts work, we show several event distributions. The energy and angular distributions for single-W’s are not changed much at LEP energies because it is produced nearly at rest due to the t -channel production. We arbitrarily take the energy point $E_{cm} = 192$ GeV. Figure 3-a) and b) compares the distribution for the invariant mass of $e^- \bar{\nu}_e$: $M(e^- \bar{\nu}_e)$ versus that of $\mu^+ \nu_\mu$: $M(\mu^+ \nu_\mu)$ with no cuts (3-a) and with the cuts stated above (3-b). Double resonant contribution is clearly suppressed by the cuts (1).

Although the single-W process dominates in the sample after the cuts (1), a small fraction of extra components exist. As is seen in figure 3-c) (the momentum of muon: P_μ) and 3-d) (P_μ versus $M(\mu^+ \nu_\mu)$), this extra contribution is distinct from the single-W production. Events with low momentum mainly come from the non-resonant diagram (the third diagram in figure 2) and the rest with high momentum are from single-W (the first 2 diagrams in figure 2). With a further requirement of $P_\mu > 20$ GeV, the single-W events can be selected. We call this set of cuts “single-W cuts”. The $M(e^- \bar{\nu}_e)$ distribution with “single-W cuts” (solid line) and with no cuts (dashed line) are compared in figure 3-e), which illustrates the rejection power against W-pair events. The angular distribution of the muon after the “single-W cuts” are shown in figure 3-f). The muon from the single-W process has high energy and its angular distribution is not particularly forward-peaked. Because of this very high Pt signature, one can remove two-photon events without significant loss of single-W events.

We have calculated the total cross-section for $e^+ e^- \rightarrow e^- \bar{\nu}_e \mu^+ \nu_\mu$ in three cases;

- With no cuts.
- “Canonical cuts” [5]: $|\cos \theta_{e^-}|, |\cos \theta_{\mu^+}| < 0.985$ and $E_{e^-}, E_{\mu^+} > 1$ GeV.
- “Single-W cuts” defined above.

Figure 4 compares the results as a function of E_{cm} . Since “canonical cuts” enhances W-pair production, the cross-section rises rapidly above the WW threshold. A monotonic increase in single-W cross-section is seen as E_{cm} increases. Taking the charge conjugate state into account, the cross-section of the single-W process with $e\nu\mu\nu$ final state is significant (table 1). One can observe “single muon” events from single-W production with modest luminosity at LEP2.

E_{cm} (GeV)	161	176	188	192
σ (fb)	28	39	50	54

Table 1: Cross-section of single-W process with $e\nu\mu\nu$ final state

4 Anomalous couplings

To test the triple gauge boson coupling, we use the following effective Lagrangian [13] assuming both C and P conservation:

$$i\mathcal{L}_{eff}^{WWV} = g_{WWV} \left[g_1^V \left(W_{\mu\nu}^\dagger W^\mu V^\nu - W_\mu^\dagger V_\nu W^{\mu\nu} \right) + \kappa_V W_\mu^\dagger W_\nu V^{\mu\nu} + \frac{\lambda_V}{m_W^2} W_{\rho\nu}^\dagger W_\nu^\mu V^{\rho\nu} \right] \quad (2)$$

where $V = \gamma$ or Z , and the overall couplings are $g_{WW\gamma} = e$, $g_{WWZ} = e \cot \theta_W$, $W_{\mu\nu} = \partial_\mu W_\nu - \partial_\nu W_\mu$ and $V_{\mu\nu} = \partial_\mu V_\nu - \partial_\nu V_\mu$.

Since g_1^V is required to be 1 by electromagnetic gauge invariance, deviations from the Standard Model are defined as 5 parameters:

$$\Delta g_1^Z \equiv (g_1^Z - 1), \quad \Delta \kappa_\gamma \equiv (\kappa_\gamma - 1), \quad \Delta \kappa_Z \equiv (\kappa_Z - 1), \quad \lambda_\gamma, \quad \lambda_Z \quad (3)$$

Current best published bounds are obtained by CDF and DØ from studies of $W\gamma$ events [14]: $-1.6 < \Delta \kappa_\gamma < 1.8$, $-0.6 < \lambda_\gamma < 0.6$.

The anomalous TGCs are already severely constrained by low energy data [15]. The parameters in equation (3) are no longer independent each other in order to protect low energy observables from acquiring discrepancies with the experimental data. Extensive studies by the symmetry requirements have been done from this point of view, which are excellently summarised in [16, 17]. In case the $SU(2)_L \times U(1)_Y$ gauge symmetry is realized linearly, only three of the five couplings are found to be independent [15, 16, 17] by considering the dimension 6 operators which do not affect the gauge boson propagators at tree level. As a result, the WWZ couplings are related to the $WW\gamma$ ones with the equations:

$$\Delta \kappa_\gamma = -\cot^2 \theta_W \cdot (\Delta \kappa_Z - \Delta g_1^Z), \quad \lambda_\gamma = \lambda_Z. \quad (4)$$

The anticipated best sensitivity from the W-pair analysis at LEP2 are inferred based on this relation, which are found to be [1]: $\Delta \kappa_\gamma = 0.06$, $\lambda_\gamma = 0.04$

and $\Delta g_1^Z = 0.02$. Another set of three parameters is relevant for the TGC studies at LEP2. For example, the set $(\Delta\kappa_\gamma, \Delta\kappa_Z, \Delta g_1^Z)$ with $\lambda_\gamma = \lambda_Z = 0$ corresponds to the nonlinear realization case with the operators of the lowest dimensionality [1, 17].

In contrast to the W-pair production, the observable of the single-W process is not constrained by these relations since the contribution from the WWZ vertex diagram for single-W process is very small at LEP energies. In figure 5, we demonstrate the variation of the cross-section at $E_{cm} = 192$ GeV as a function of the anomalous couplings; λ_γ (a), $\Delta\kappa_\gamma$ (b), λ_Z (c), $\Delta\kappa_Z$ (d) and Δg_1^Z (e), respectively. The cross-section depends only marginally on WWZ related couplings while we see a large sensitivity to $WW\gamma$ ones. Because of this orthogonal feature against WWZ couplings, one can extract anomalous $WW\gamma$ couplings independently by studying the single-W process even without using any relationship between $WW\gamma$ and WWZ couplings.

Figure 6 shows the similar sensitivity curves to figure 5 but the constraint (4) is used. The difference between two cases is numerically very small. For the rest of this paper, we adopt the constraint (4) in order to preserve the gauge invariance. The third independent quantity Δg_1^Z is also insensitive to the observable and only a huge deviation from the Standard Model could give rise to a detectable change of the cross-section. Therefore we approximate it to the Standard Model value ($=0$).

Figure 7-a), b) and c) illustrate a specific sensitivity to the anomalous coupling as a function of E_{cm} . In figure 7-a), the solid line corresponds to the Standard Model cross-section with “single-W” cut. If we assume anomalous couplings to be $\Delta\kappa_\gamma = -\cot^2\theta_W \cdot \Delta\kappa_Z = 2$, we get a significantly larger cross-section (dashed line). Also in the figure, the ratio of two cases (b) and the difference between two (c) are shown as a function of E_{cm} . The enhancement factor of about 6 is expected, which is in marked contrast to W-pair production since the measurement of the WW total cross-section is not sensitive to the anomalous coupling around the LEP energy region. We give the sensitivity for W-pair production as dashed lines in figure 7-b) and c), where the “canonical cuts” are made to enhance WW contribution above the threshold. The W-pair case is much less sensitive than the single-W case.

We estimate the precision in TGCs based on a 1-parameter fit. The anticipated sensitivity for the anomalous couplings are;

$$-0.4 < \Delta\kappa_\gamma < 0.3, \quad -0.9 < \lambda_\gamma < 1.0,$$

at 95% C.L., where $E_{cm} = 192$ GeV and $\int \mathcal{L} dt = 500\text{pb}^{-1}$ are assumed.

We emphasise that one can improve the limits further by including other channels: $e\nu_e e\nu_e$, $e\nu_e \tau\nu_\tau$ and $e\nu_e q\bar{q}'$. Event signatures for the other lepton channels are similar to single muon case. The hadronic channel might be difficult to separate from γZ^0 events where the initial γ escapes down the beam pipe. Since a single-W is produced nearly at rest, two jets from the W tend to be back-to-back and the direction of missing energy does not necessarily lie close to the beam pipe. This signature may help for the separation from the γZ^0 process. In view of TGC studies, the hadronic single-W channel is very attractive because of its large cross-section. We have calculated the total cross-section for the hadronic channel to be 350fb at $E_{cm} = 192$ GeV. Single-W process is, in general, more sensitive to $\Delta\kappa_\gamma$ than to λ_γ . Although the anticipated bound on λ_γ will not be attractive (~ 0.6), the sensitivity of $|\Delta\kappa_\gamma| \sim 0.1$ is expected with $\int \mathcal{L} dt = 500\text{pb}^{-1}$ which is comparable to that will be obtained from W-pair studies [1].

5 Conclusion

We have for the first time presented the TGC studies making use of single-W production at the LEP energy region. The cross-section measurement of this process are found to give good sensitivities to the anomalous couplings, in particular to $\Delta\kappa_\gamma$.

We emphasise that the precise study of the $WW\gamma$ vertex from $e^+e^- \rightarrow e^-\bar{\nu}_e W^+$ process is important to disentangle the complex effects coming from $WW\gamma$ and WWZ vertices which will be obtained from W-pair production analyses. In this sense, the bounds from single-W process are complementary to W-pair ones.

It should also be noted that the sensitivity for the anomalous couplings does not depend so much on E_{cm} since the cross-section of the single-W process is relatively flat over the LEP energy region while the considerable enhancement is expected with small deviations from the Standard Model. Data collected at any energy points are equally useful. This signature is in contrast to the W-pair production analysis, which depends largely on the E_{cm} available. Especially even below WW threshold, single-W analysis has a sensitivity to the anomalous couplings. For example, each LEP experiment has already collected 5pb^{-1} data at 130-136 GeV. Searching for high

Pt muons would already give $\mathcal{O}(10)$ sensitivity to the anomalous coupling constants.

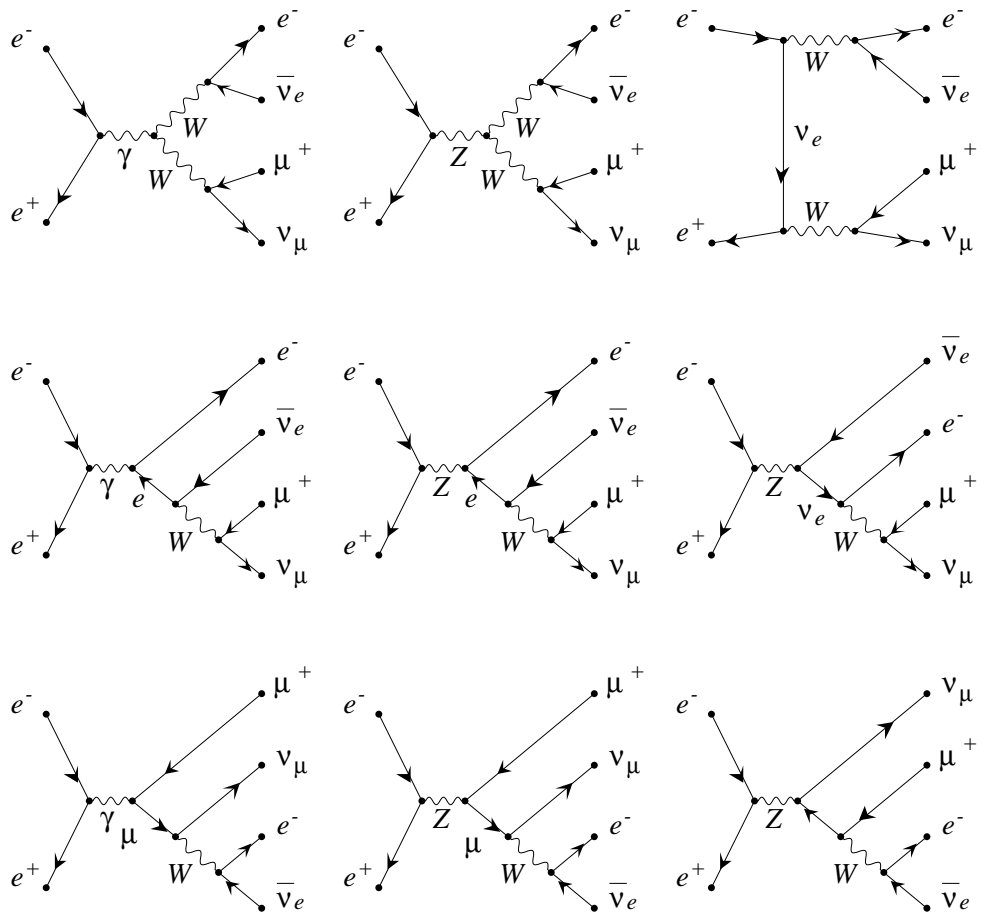
Acknowledgements

The authors would like to thank Minami-Tateya theory group of KEK, especially Y. Shimizu, J. Fujimoto and T. Ishikawa for their physics discussions and technical help in grc4f system. We also wish to thank T. Kawamoto for his intuitive discussions and suggestions at the initial stage of this work. We are grateful to P. Watkins for his proofreading the manuscript which improved the English very much. This work was supported in part by Japan Society for Promotion of Science under Fellowship for Research Program at Centres of Excellence Abroad.

References

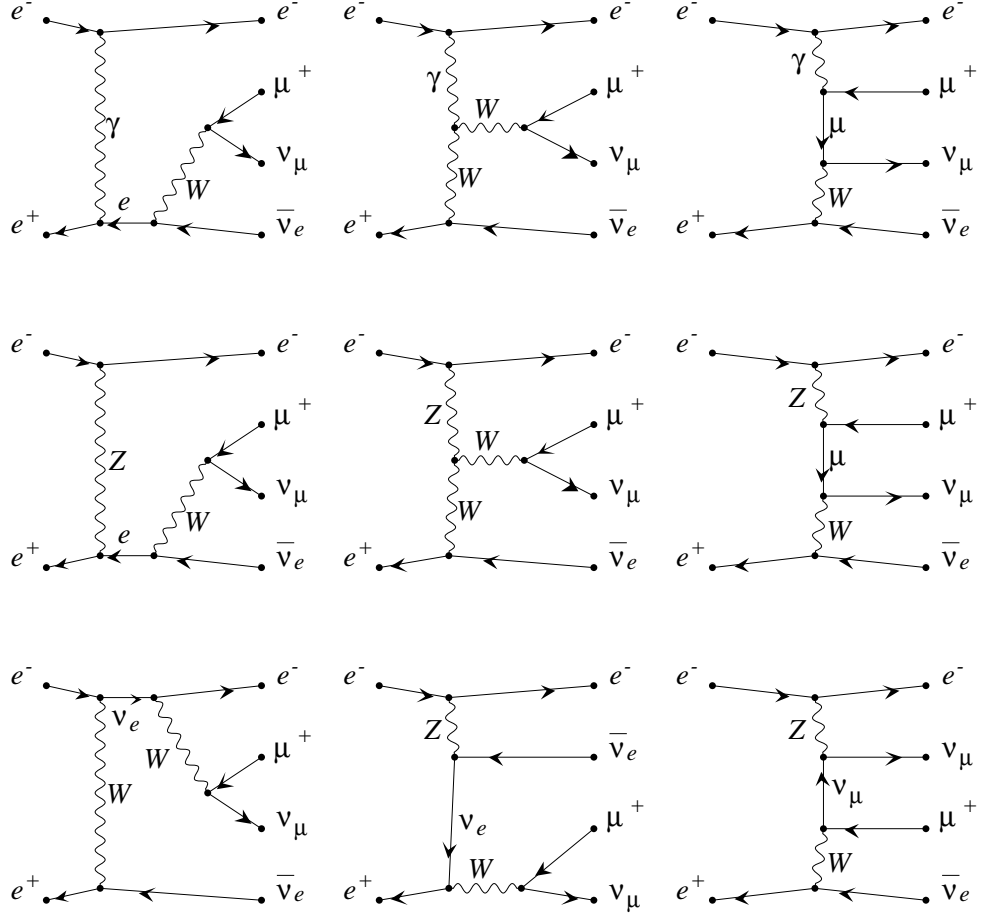
- [1] G. Gounaris *et al.*, ‘Triple gauge boson couplings’ in *Physics at LEP2*, ed. G. Altarelli *et al.*, vol. 1, p.525, CERN 96-01, February 1996 and hep-ph/9601233, and references there in.
- [2] G. Couture and S. Godfrey, Phys. Rev. **D50** (1994) 5607.
- [3] K.J. Abraham, J. Kalinowski, P.Śaciepko, Phys. Lett. **B339** (1994) 136.
- [4] E.N. Argyres and C.G. Papadopoulos, Phys. Lett. **B263** (1991) 298; C.G. Papadopoulos, Phys. Lett. **B333** (1994) 202; C.G. Papadopoulos, Phys. Lett. **B352** (1995) 144.
- [5] D. Bardin *et al.*, ‘Event generators for WW physics’ in *Physics at LEP2*, ed. G. Altarelli *et al.*, vol. 2, p.3, CERN 96-01, February 1996.
- [6] A. Aeppli, F. Cuypers and G.J. van Oldenborgh, Phys. Lett. **B349** (1993) 413; E.E Boos *et al.*, Phys. Lett. **B326** (1994) 190.
- [7] Y. Kurihara, D. Perret-Gallix and Y. Shimizu, Phys. Lett. **B349** (1995) 367.
- [8] E.N. Argyres *et al.*, Phys. Lett. **B358** (1995) 339; W. Beenakker *et al.*, ‘WW cross-sections and distributions’ in *Physics at LEP2*, ed. G. Altarelli *et al.*, vol. 1, p.79, CERN 96-01, February 1996 and hep-ph/9602351.
- [9] J. Fujimoto *et al.*, ‘grc4f v1.1: a Four-fermion Event Generator for e^+e^- Collisions’, preprint KEK-CP-046 and hep-ph/9605312, and references there in.
- [10] H. Tanaka, Comput. Phys. Commun. **58** (1990) 153; H. Tanaka, T. Kaneko and Y. Shimizu, Comput. Phys. Commun. **64** (1991) 149.
- [11] S. Kawabata, Comput. Phys. Commun. **41** (1986) 127.
- [12] A.E. Kuraev, V.S. Fadin, Sov. J. Nucl. Phys. **41** (1985) 466.

- [13] K. Hagiwara, K. Hikasa, R.D. Peccei, D. Zeppenfeld, Nucl. Phys. **B282** (1987) 253;
K. Gaemers and G. Gouraris, Z. Phys. **C1** (1979) 259.
- [14] CDF Collaboration, F. Abe *et al.*, Phys. Rev. Lett. **75** (1995) 1017; DØ Collaboration, S. Adachi *et al.*, Phys. Rev. Lett. **75** (1995) 1034.
- [15] A. De Rújula, M.B. Gavela, P. Hernández and E. Massó, Nucl. Phys **B384** (12992) 3;
K. Hagiwara, S. Ishihara, R. Szalapski and D. Zappendorf, Phys. Rev. **D48** (1993) 2182.
- [16] M. Bilenky, J.L. Kneur, F.M. Renard and D. Schildknecht, Nucl. Phys. **B409** (1993) 22;
H. Aihara *et al.*, FERMILAB-Pub-95/031.
- [17] F. Boudjema, Proceedings of the “Workshop on Physics and Experiments with Linear e^+e^- Colliders”, eds. F.A. Harris *et al.*, World Scientific, 1994, p.712.



produced by GRACEFIG

Figure 1: The s -channel diagrams of the $e^+e^- \rightarrow e^-\bar{\nu}_e\mu^+\nu_\mu$ process in the unitary gauge. The first three diagrams in the first row are double-resonant diagrams.



produced by GRACEFIG

Figure 2: The t -channel diagrams of the $e^+e^- \rightarrow e^-\bar{\nu}_e\mu^+\nu_\mu$ process in the unitary gauge. The first and second columns show the single-resonant diagrams and the rest shows the non-resonant diagrams. Diagrams in the first row (γ - W processes) gives the dominant contribution among the t -channel diagrams.

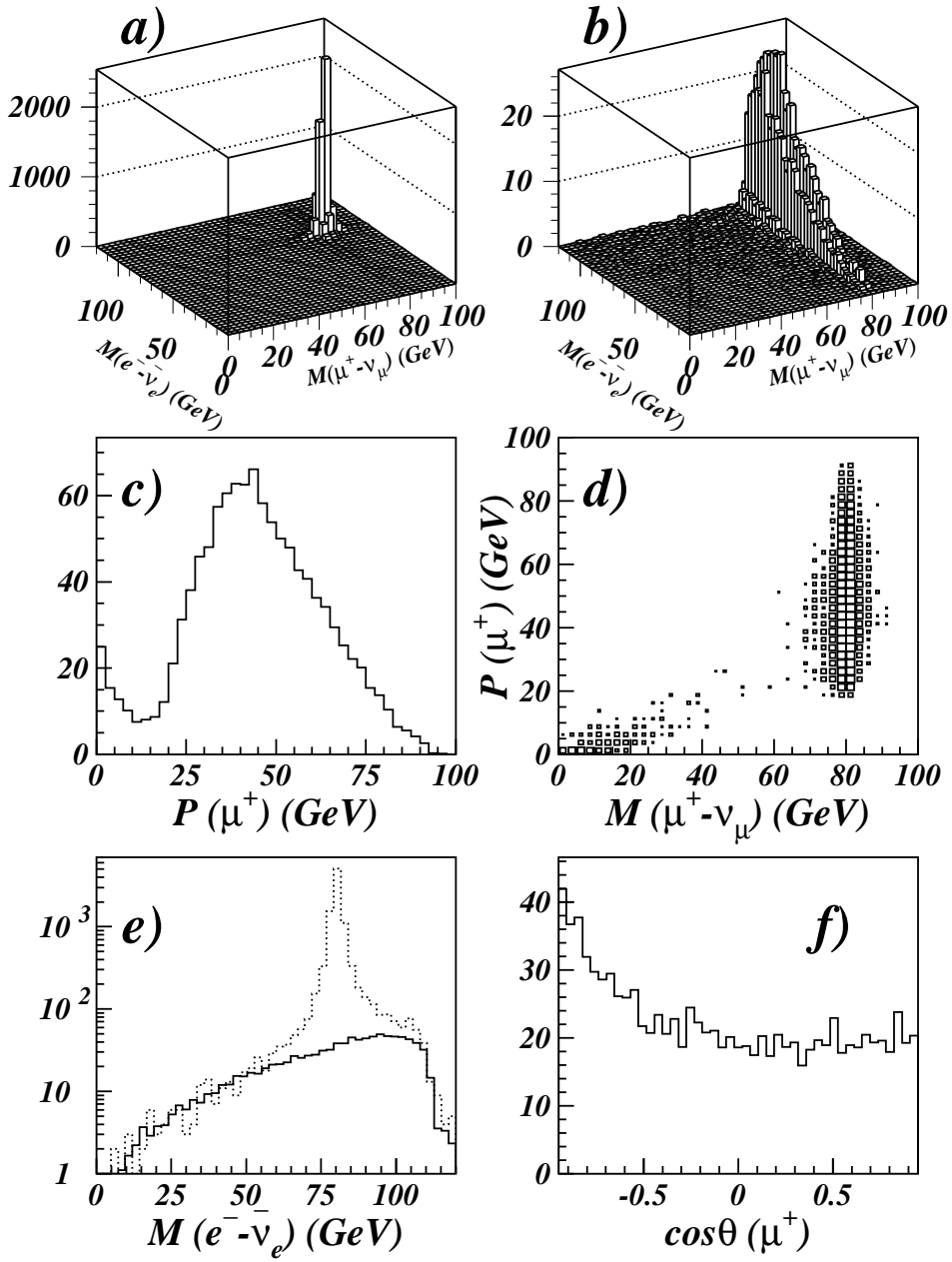


Figure 3: Event distributions for $e^+e^- \rightarrow e^-\bar{\nu}_e\mu^+\nu_\mu$ process. The top two figures compares $M(e^- - \bar{\nu}_e)$ versus $M(\mu^+ - \nu_\mu)$ with no cuts (a) and with the cuts-(1) (b). Figure c) and d) show the momentum distribution for muons. The W-pairs (dashed line in e) are highly suppressed by “single-W cut”, while keeping single-W contribution (solid line in e). The angular distribution for muon is given in f).

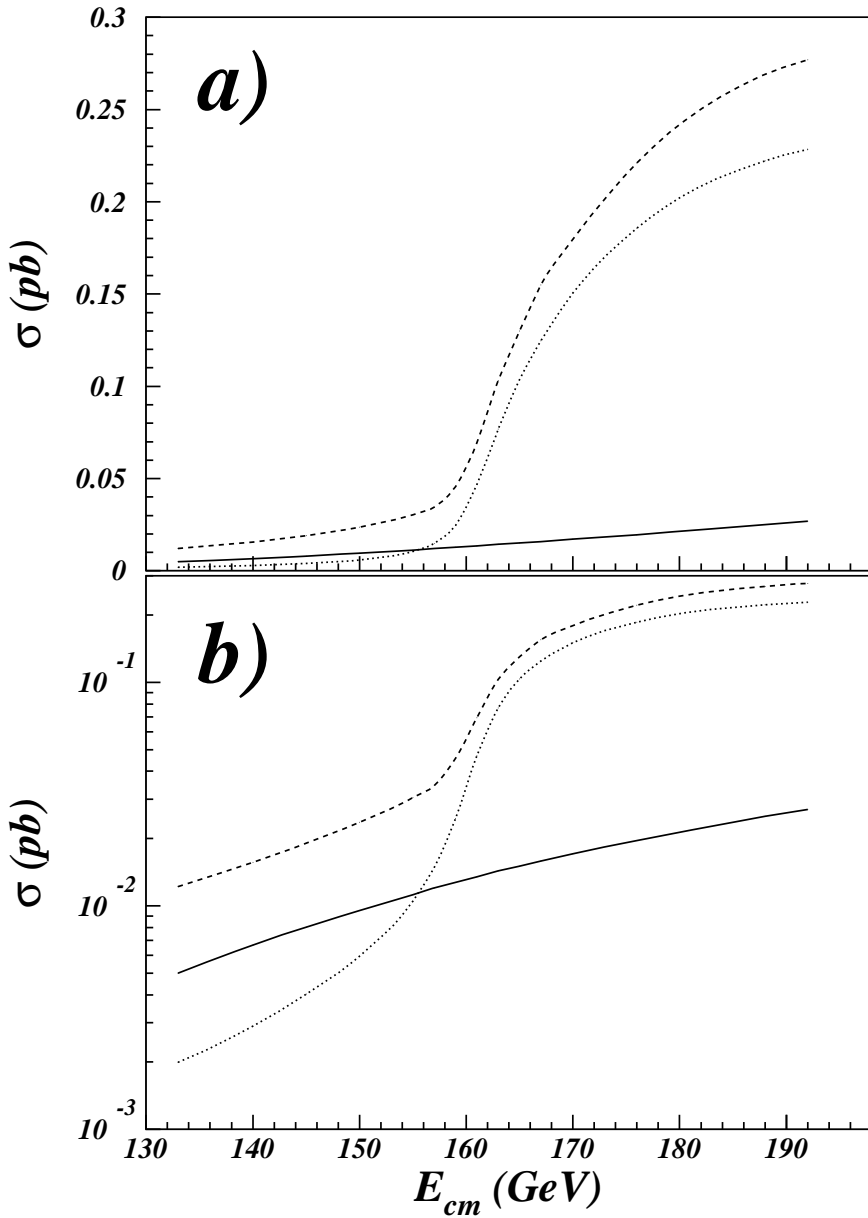


Figure 4: The total cross-section for the process $e^+e^- \rightarrow e^-\bar{\nu}_e \mu^+\nu_\mu$ as a function of E_{cm} with no cut (dashed line), with “canonical cuts” (dotted line) and with “single-W cuts” (solid line) on a linear scale (a) and a logarithmic scale (b).

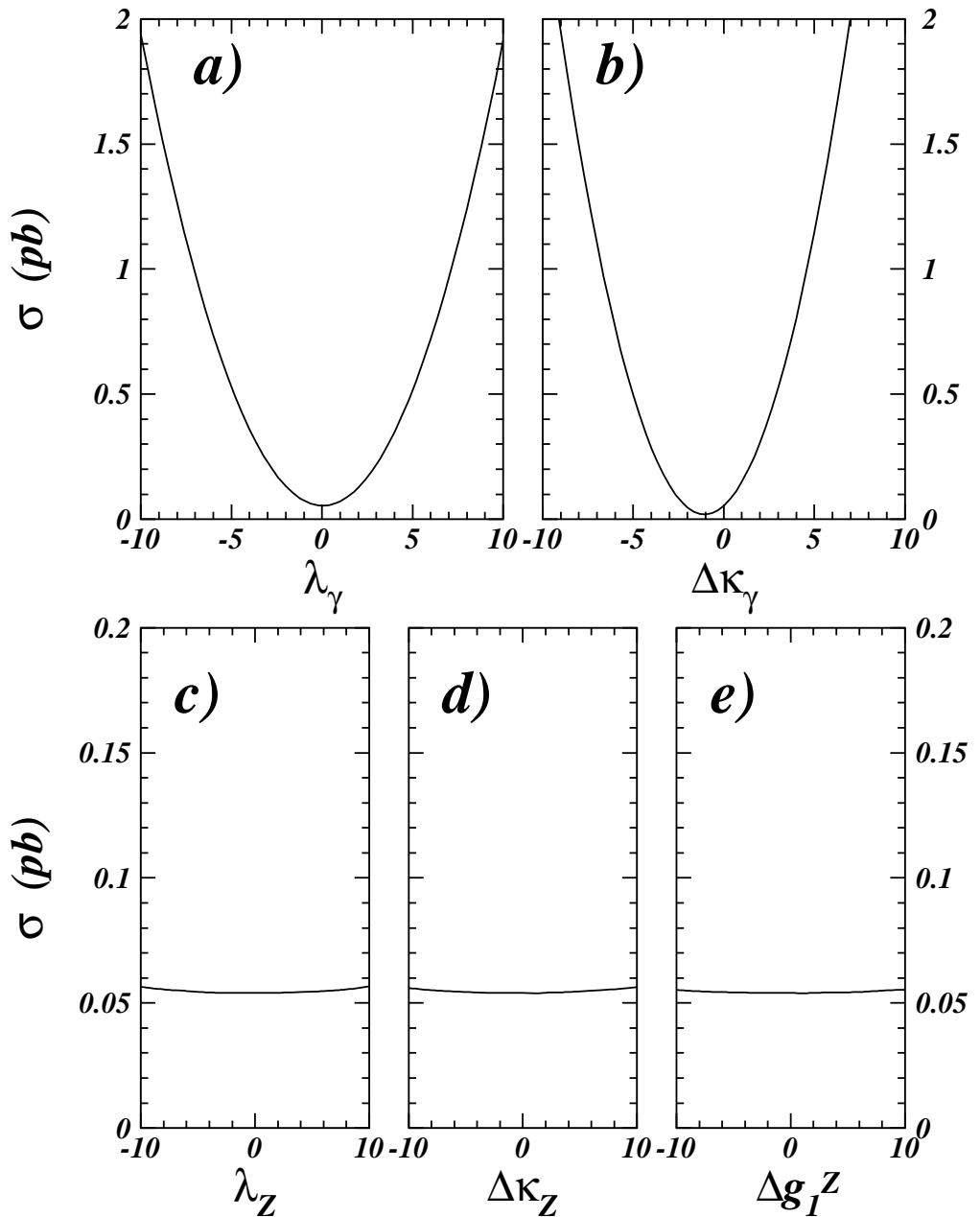


Figure 5: Variation of the cross-section for the single-W process with $e\nu\mu\nu$ final state at $E_{cm} = 192$ GeV: (a) λ_γ , (b) $\Delta\kappa_\gamma$, (c) λ_Z , (d) $\Delta\kappa_Z$ and (d) Δg_1^Z . Note that the vertical scales are expanded for Z-related couplings (c-e).

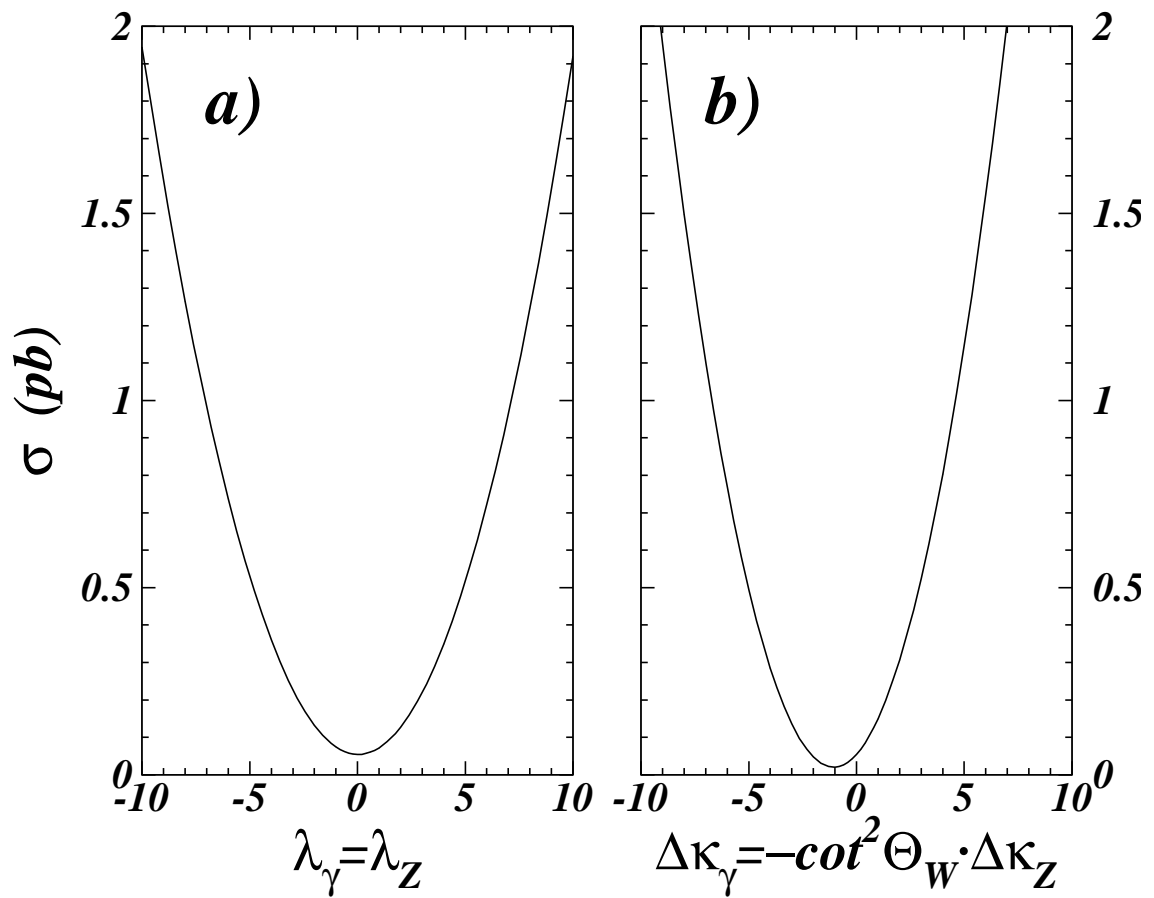


Figure 6: Variation of the cross-section for the single-W process with $e\nu\mu\nu$ final state at $E_{cm} = 192$ GeV with $SU(2) \times U(1)$ constraints: (a) $\lambda_\gamma = \lambda_Z$, (b) $\Delta\kappa_\gamma = -\cot^2\theta_W \cdot \Delta\kappa_Z$.

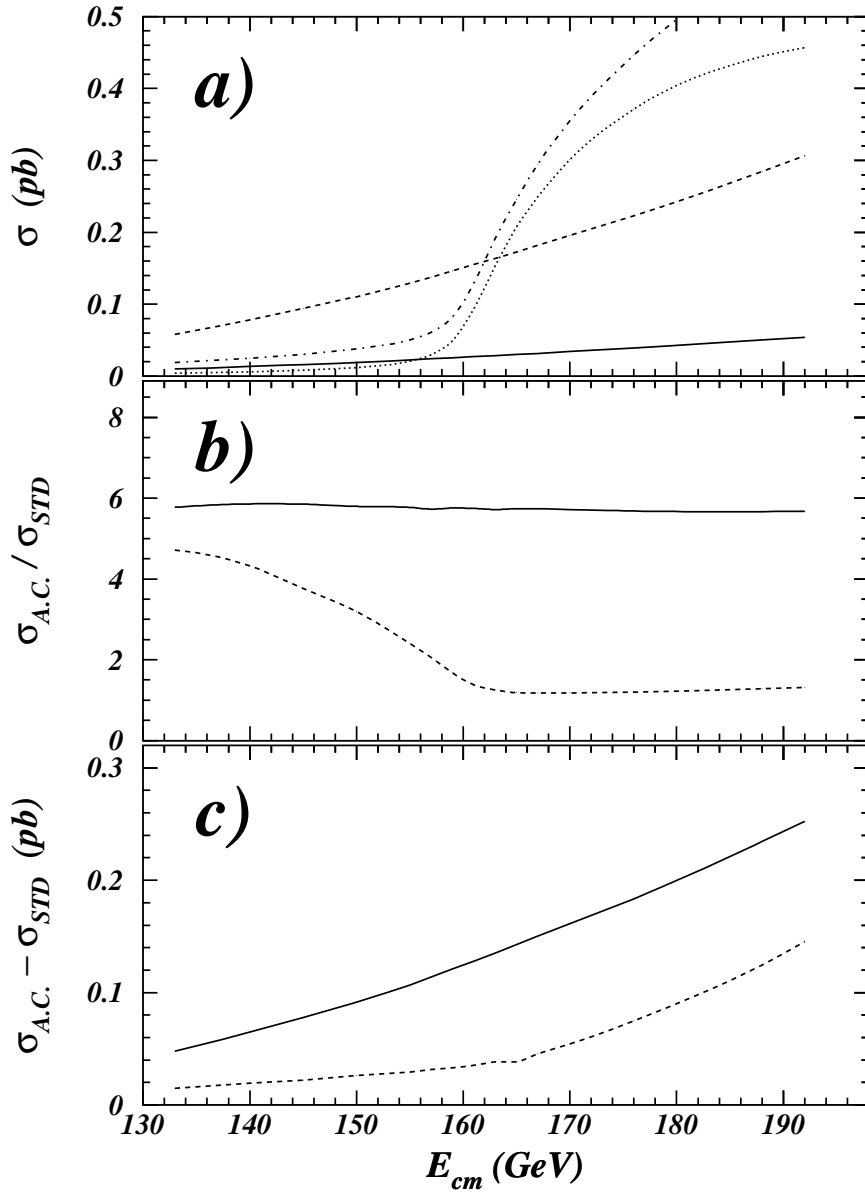


Figure 7: The enhancement of the cross-section due to the anomalous couplings as a function of E_{cm} . Two cases are compared: “single-W cuts” and “canonical cuts”. In the cross-section plot (a), solid (single-W) and dotted (canonical) line correspond to the Standard Model cross-section (σ_{STD}), and dashed (single-W) and dashed-dotted (canonical) line is with the assumption of $\Delta\kappa_\gamma = -\cot^2\theta_W \cdot \Delta\kappa_Z = 2$ ($\sigma_{A.C.}$). The ratios of σ_{STD} and $\sigma_{A.C.}$ are given (b) as well as the differences (c) (solid line: single-W cut, dashed-line: canonical cut).